

# The Quantitative Effect of Mo and Cu on the Stress Corrosion Cracking and Pitting Corrosion Behavior of Ultra-Pure Ferritic Stainless Steels

Weiwei Wu<sup>1,2</sup>, Yanjun Guo<sup>1</sup>, Haifeng Yu<sup>2</sup>, Yiming Jiang<sup>1</sup>, Jin Li<sup>1,\*</sup>

<sup>1</sup> Department of Materials Science, Fudan University, Shanghai 200433, China

<sup>2</sup> Research and Development Center, Baosteel Co., Ltd., Shanghai 201900, PR China

\*E-mail: [corrosion@fudan.edu.cn](mailto:corrosion@fudan.edu.cn)

Received: 2 September 2015 / Accepted: 10 October 2015 / Published: 4 November 2015

---

The quantitative effect of Mo and Cu on the stress corrosion cracking and the pitting corrosion of ultra-pure ferritic stainless steel has been studied by immersion tests in 42 wt.% MgCl<sub>2</sub> boiling solution, cyclic salt spray test, polarization curves and FeCl<sub>3</sub> immersion test. The results showed that the steels could be immune to the stress corrosion cracking failure with Mo and Cu content both less than 0.4 wt.%. The specimens containing more than 0.8 wt.% Mo and 0.2 wt.% Cu were sensitive to the stress corrosion cracking. The surface morphology of the cracked steels after stress corrosion cracking tests was featured by a mixture of intergranular and transgranular fracture, but mostly transgranular fracture. With the more addition of Mo and Cu, the stress corrosion cracking sensitivity grew higher. The quantitative effect of Mo and Cu addition on the stress corrosion cracking of ultra-pure ferritic stainless steel was given in a whole graph and the synergetic effect of Mo and Cu elements on the stress corrosion cracking was discussed. Besides, it was found that the Mo element increased the pitting corrosion resistance in the chloride containing environment. However, the addition of Cu reduced the pitting corrosion resistance of ultra-pure ferritic stainless steel, which might be attributed to the precipitation of  $\epsilon$ -Cu phase.

---

**Keywords:** Stainless steel; Stress corrosion cracking; Pitting corrosion

## 1. INTRODUCTION

Ultra-pure ferritic stainless steels (FSSs) have attracted great attention due to their distinct advantages such as higher stress corrosion cracking (SCC) resistance and lower cost as compared to the austenite stainless steels [1-6]. In the ultra-pure FSSs, molybdenum (Mo) is considered as a strong ferrite forming element, which is related to the solid solution strengthening effect. Copper (Cu) is used

as a minor alloying element in the ferrite matrix. The ultra-pure FSSs can be widely used in extensive fields such as automobile exhaust systems, solar water heater, containers, and buses. However, these materials may suffer from the stress corrosion cracking and the pitting corrosion in some aggressive environments during the service [1].

The stress corrosion cracking and the pitting corrosion are two of the most important localized corrosion attacks, which are resulted from a combination of metallurgical and environmental factors such as the alloying elements, the complex interplay of metal, interface and environmental properties [7-9]. The effect of Mo and Cu additions on the corrosion resistance of FSSs has been widely studied, and the role of the Mo and Cu elements is complex [10-14]. On one hand, previous studies found that the alloying elements including Mo and Cu had a beneficial effect on the corrosion resistance of stainless steels [10-14]. The addition of Mo could enhance the repassivation ability of the passive film or reduce the anodic dissolution rate inside the pit holes, and thus could improve the pitting corrosion resistance [10-14]. In sulfuric acid solutions, the addition of Cu elements in stainless steels could result in the Cu enrichment in the surface film, which could suppress the anodic dissolution and improve the pitting corrosion resistance through the redeposition of previously dissolved copper [15-21]. However, on the other hand, Mo has been found to be harmful to the intercrystalline corrosion resistance of stainless steels. Schwind et al. [22] reported that Mo could accelerate the formation of  $\delta$  phase and  $M_{23}C_6$  at the boundaries of stainless steels, which could increase its intercrystalline corrosion sensibility. Seo et al. [23] reported that Cu alloying element in the ferritic stainless steel resulted in a detrimental effect on the stability of the passive film in the sulfuric acid media. Ujiro et al. [20] reported that the protective effect of the Cu on the active surface in acidic chloride solution was less effective because the presence of  $Cl^-$  ions decreased the stability of the deposits.

However, to date, little research has been reported about the synergistic effect of Mo and Cu on the SCC of ultra-pure ferritic stainless steels. In Jun Shu's study, the effect of Mo and Cu addition on the SCC has been clarified; however, the influence wasn't quantitatively analyzed [24]. It is important to quantitatively reveal the synergistic effect of Mo and Cu on the SCC behaviour of ultra-pure ferritic stainless steels, which can help researchers design new stainless steels with perfect stress corrosion resistance through selecting the appropriate amount of Mo and Cu addition. In this study, ultra-pure ferritic stainless steels with various Mo and Cu addition were produced, and then the SCC sensitivities and pitting corrosion resistance were studied. As a result, the quantitative effect of Mo and Cu addition on the SCC resistance was discussed.

## 2. MATERIALS AND METHODS

### 2.1 Materials

In this study, to quantitatively characterize the effects of Cu and Mo addition on the resistance to SCC and pitting corrosion of ferritic stainless steels, ultra-pure Cr ferritic stainless steels with different Mo and Cu contents but similar other contents were designed, of which twenty possible sets of Cu and Mo content (wt.%) were shown in Table 1. The sequence between batches was from I to III

and the sequence between the samples in a batch was from A to H. To optimize the test plan and minimize the amount of smelted steels, eight kinds of specimens including I<sub>A</sub>, I<sub>B</sub>, I<sub>C</sub>, II<sub>A</sub>, II<sub>B</sub>, II<sub>G</sub>, II<sub>H</sub> and III<sub>H</sub> were smelted. There were twelve materials, i.e. I<sub>D</sub>, II<sub>C</sub>, II<sub>D</sub>, II<sub>E</sub>, II<sub>F</sub>, III<sub>A</sub>, III<sub>B</sub>, III<sub>C</sub>, III<sub>D</sub>, III<sub>E</sub>, III<sub>F</sub> and III<sub>G</sub> were just designed not smelted, as shown in Table 1 with a mark of “\*”. The relative chemical composition of eight smelted materials was shown in Table 2. These steels were produced from 150 kg high vacuum-melted ingots and hot rolled to 4 mm thick sheets and then cold rolled to 1 mm thick sheets with intermediate annealing and pickling.

## 2.2 Stress corrosion cracking tests

Stress corrosion was the main research of this paper. The research method was an immersing test according to the ASTM G36-94(2000) standard [25]. Eight specimens including I<sub>A</sub>, I<sub>B</sub>, I<sub>C</sub>, II<sub>A</sub>, II<sub>B</sub>, II<sub>G</sub>, II<sub>H</sub> and III<sub>H</sub> were prepared for each experiment. The geometry of specimens for stress corrosion cracking experiments was as follows: the gauge length was 75 mm, the width 10 mm and the thickness 1.0 mm. There were two holes centrally located at the left and right edge of the specimens, respectively. The diameter of the two holes was 4.5 mm, and the distance between the center of hole and the edge of specimens was 4.75 mm. According to the ASTM G30-97 (2009) standard [26], the stress corrosion samples was bend into a U-shaped with a diameter of 16 mm roller die, with their arms parallel to the fastening bolt. Stress corrosion solution was 42 wt.% boiling MgCl<sub>2</sub> solutions, with the boiling point of  $143 \pm 1$  °C. The samples were immersed in the solutions for 1 month. During this period, the samples were examined every 30 minutes. If SCC was observed, the test was ended and the time for SCC was recorded as the most important SCC resistance evaluation parameter about the sample. If no stress corrosion cracking occurred after 1 month, the test was ended and the material was determined as immune to SCC.

## 2.3 Pitting corrosion analysis

Cyclic salt spray test, polarization curves and FeCl<sub>3</sub> immersion test were used to investigate the pitting corrosion resistance of ultra-pure ferritic stainless steels.

Cyclic salt spray test was performed according to the Chinese national GB/T 20854-2007 standard [27]. The electrolyte for this test was 5 wt.% NaCl solution according to the GB standard. The single cycle was chosen as 2 h of salt spray, 4 h dry exposure and 2 h of wet exposure. After each 80 h exposure period, the panels were rinsed and visually examined for the presence of any corrosion, blistering, softening, staining, or other film defects and repositioned with the exposure cabinet to ensure uniformity of exposure conditions. The panel were exposed for a total of 240 h and examined for corrosion.

For the polarization test, the working electrodes for electrochemical measurement were embedded in epoxy resin leaving a working area of  $1.0 \times 1.0$  cm<sup>2</sup>. All the tests were carried out in 3.5 wt.% NaCl solutions at room temperature. The electrochemical measurements were performed in a conventional three-electrode cell. The ultra-pure ferritic stainless steels were used as the working

electrode, a platinum sheet as the counter electrode, and a saturated calomel electrode (SCE) as the reference electrode. Prior to polarization measurements, working electrodes were initially reduced potentiostatically at  $-0.9 V_{SCE}$  for 3 min to remove the air-formed oxides that might be present. The corrosion potential was then recorded for 10 min to achieve a stable open circuit potential. The polarization curves were measured potentiodynamically from  $-0.25 V$  (vs. open circuit potential  $E_{ocp}$ ) to the trans-passive region with a scanning rate of  $1.667 mV/s$ .

$FeCl_3$  immersion tests were carried out in 6 wt.%  $FeCl_3$  solution at  $35\text{ }^\circ C$  open to air according to the ASTM G48-03(2003) standard [28]. Before the experiment, the samples were cut into  $30 \times 20$  mm and polished to 600#, and measured and weighted to a precision of 0.01 mg. After 24 h immersion, the samples were extracted, cleaned with water and then weighted again at room temperature. The corrosion rate of specimens after immersion was calculated according to the formula below:

$$Corrosion\ rate = \frac{w_1 - w_2}{s \times t}$$

$w_1$  — The weight of the specimens before the immersion test.

$w_2$  — The weight of the specimens after the immersion test.

$s$  — The total surface area of the specimens.

$t$  — The duration of test.

### 2.4 Corrosion morphology analysis

The optical image of corroded specimens was examined using camera after SCC tests. The surface morphology of corroded specimens was observed by scanning electron microscopy (SEM).

**Table 1.** Cu and Mo composition of ultra-pure ferritic stainless steels (wt.%)

Cu Mo	0	0.1	0.2	0.4
0	III <sub>D</sub> <sup>*</sup>	III <sub>C</sub> <sup>*</sup>	III <sub>B</sub> <sup>*</sup>	III <sub>A</sub> <sup>*</sup>
0.4	II <sub>D</sub> <sup>*</sup>	II <sub>C</sub> <sup>*</sup>	II <sub>B</sub>	II <sub>A</sub>
0.8	I <sub>D</sub> <sup>*</sup>	I <sub>C</sub>	I <sub>B</sub>	I <sub>A</sub>
1.2	II <sub>H</sub>	II <sub>G</sub>	II <sub>F</sub> <sup>*</sup>	II <sub>E</sub> <sup>*</sup>
1.5	III <sub>H</sub>	III <sub>G</sub> <sup>*</sup>	III <sub>F</sub> <sup>*</sup>	III <sub>E</sub> <sup>*</sup>

\*-These materials are just designed not smelted.

**Table 2.** Chemical compositions of the ultra-pure ferritic stainless steels (wt.%).

Material	C	Si	Mn	S	P	Cr	Ni	Mo	Cu	N
I <sub>A</sub>	0.0058	0.21	0.22	0.001	0.021	21.2	0.18	0.79	0.36	0.0072
I <sub>B</sub>	0.0068	0.21	0.21	0.001	0.013	21.8	0.2	0.77	0.22	0.0075
I <sub>C</sub>	0.0063	0.21	0.22	0.001	0.015	21.6	0.18	0.78	0.11	0.0077

II <sub>A</sub>	0.006	0.19	0.22	0.001	0.02	21.36	0.18	0.42	0.39	0.0064
II <sub>B</sub>	0.006	0.25	0.12	0.004	0.011	21.41	0.19	0.41	0.18	0.009
II <sub>G</sub>	0.0055	0.21	0.22	0.001	0.015	21.67	0.19	1.18	0.12	0.0067
II <sub>H</sub>	0.0040	0.22	0.19	0.002	0.02	21.96	0.25	1.19	0.02	0.0065
III <sub>H</sub>	0.004	0.22	0.19	0.002	0.02	21.96	0.25	1.48	0.02	0.0065

### 3. RESULTS AND DISCUSSION

#### 3.1 Effect of Mo and Cu on SCC of ultra-pure ferritic stainless steels

To quantitatively characterize the effects of Mo and Cu addition on the SCC resistance of ultra-pure ferrite stainless steels, the SCC resistance was evaluated by means of the 42 wt.% boiling MgCl<sub>2</sub> solution immersing test as mentioned in 2.2 and the SCC results of these steels were listed in Table 3.

##### 3.1.1 Results of SCC corrosion tests for the FSS with 0.8 wt.% Mo

To initially quantitatively characterize the effects of Mo and Cu addition on the SCC resistance of ultra-pure ferritic stainless steels, three ferritic stainless steels I<sub>A</sub>, I<sub>B</sub> and I<sub>C</sub> with 0.8 wt.% Mo but different Cu contents were measured.

**Table 3.** The SCC test results of ultra-pure ferritic stainless steels

Material	SCC time / h	Material	SCC time / h
I <sub>A</sub>	4-6	II <sub>G</sub>	10-12
I <sub>B</sub>	7-8	II <sub>H</sub>	>720
I <sub>C</sub>	>720	III <sub>A</sub> *	>720*
I <sub>D</sub> *	>720*	III <sub>B</sub> *	>720*
II <sub>A</sub>	>720	III <sub>C</sub> *	>720*
II <sub>B</sub>	>720	III <sub>D</sub> *	>720*
II <sub>C</sub> *	>720*	III <sub>E</sub> *	<24*
II <sub>D</sub> *	>720*	III <sub>F</sub> *	<24*
II <sub>E</sub> *	<24*	III <sub>G</sub> *	<24*
II <sub>F</sub> *	<24*	III <sub>H</sub>	>720

\*-The result is from analyzing instead of experiment.

The SCC resistance of specimens was evaluated by immersion in the 42 wt.% boiling MgCl<sub>2</sub> solution and the SCC results of these steels were listed in Table 3. It could be seen that the SCC time of I<sub>A</sub> steel with 0.4 wt.% Cu was 4–6 h, for I<sub>B</sub> steel with 0.2 wt.% Cu 7–8 h, suggesting significantly low SCC resistance for specimens I<sub>A</sub> and I<sub>B</sub>. As the Cu content in the FSS specimen decreased to 0.1 wt.% (i.e., specimen I<sub>C</sub>), no SCC was observed after 720 h immersion test.

Although four materials with 0.8 wt.% Mo and several Cu composition were concerned, only three of them were tested. It could be concluded that the Cu addition was harmful to the SCC resistance, and thus it could be deduced that the 0.8 wt.% Mo steel without Cu (i.e., specimen I<sub>D</sub>) would be immune to SCC.

Based on the above results, for ultra-pure ferritic stainless steels containing 0.8 wt.% Mo, the addition 0.2 wt.% or more Cu could cause SCC failure; however, the addition of 0.1 wt.% Cu had no harm for the SCC resistance. Therefore, the critical value of the Cu addition was 0.1 wt.% for ultra-pure ferritic stainless steels with 0.8 wt.% Mo.

### 3.1.2 The SCC corrosion tests results for the FSS with 0.4 wt.% Mo or 1.2 wt.% Mo

To further quantitatively characterize the synergetic effect of Mo and Cu addition on the SCC resistance of ultra-pure ferritic stainless steels, II<sub>A</sub>, II<sub>B</sub>, II<sub>G</sub> and II<sub>H</sub> were tested by immersion in 42 wt.% MgCl<sub>2</sub> boiling solution. The chemical compositions of the specimens were shown in Table 2. Table 3 displayed the SCC results of these steels. It could be seen that there were no SCC phenomena occurred on II<sub>A</sub> steel with 0.4 wt.% Mo and 0.4 wt.% Cu, and II<sub>B</sub> steel with 0.4 wt.% Mo and 0.2 wt.% Cu after 720 h test. For specimen II<sub>G</sub> with 1.2 wt.% Mo and 0.1 wt.% Cu, the SCC time was 10–12 h; however, for II<sub>H</sub> steel with 1.2 wt.% Mo but without Cu addition, no SCC cracks could be found on the maximum stress area after 720 h tests, suggesting that the addition of Cu had a detrimental effect on the SCC resistance for the steel with 1.2 wt.% Mo.

For ultra-pure ferritic stainless steels containing 0.4 wt.% Mo, no negative effects of the 0.4 wt.% Cu addition (i.e., specimen II<sub>A</sub>) and the 0.2 wt.% Cu addition (i.e., specimen II<sub>B</sub>) on the SCC resistance were found, which suggested that the addition of less than 0.2 wt.% Cu (i.e., specimens II<sub>C</sub> and II<sub>D</sub>) had no harm for SCC. However, for the steel with 1.2 wt.% Mo steel and 0.1 wt.% Cu content (i.e., specimen II<sub>G</sub>), it could cause SCC failure, suggesting that the steels with addition of Cu beyond 0.1 wt.% (i.e., specimens II<sub>E</sub> and II<sub>F</sub>) were susceptible to SCC failure. Besides, the steel with 1.2 wt.% Mo and without Cu (i.e., specimen II<sub>H</sub>) was immune to the SCC in the present work.

### 3.1.3 The SCC corrosion tests results for the FSS without Mo or with 1.5 wt.% Mo

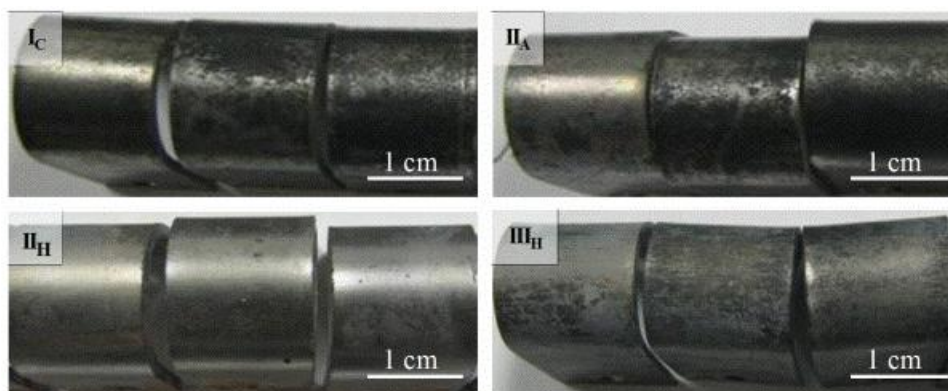
For FSS steel with 1.5 wt.% Mo, specimen III<sub>H</sub> without Cu was smelted and tested in 42 wt.% MgCl<sub>2</sub> boiling solution. As shown in Table 3, no SCC was found for the specimen III<sub>H</sub>.

Table 3 compared the SCC results of specimens between II<sub>C</sub> (0.1 wt.% Cu and 0.4 wt.% Mo), I<sub>C</sub> (0.1 wt.% Cu and 0.8 wt.% Mo) and II<sub>G</sub> (0.1 wt.% Cu and 1.2 wt.% Mo). It is seen that when the content of Cu was 0.1 wt.%, the SCC resistance was similar for specimens as the Mo content increased from 0.4 wt.% to 0.8 wt.%. However, as the content of Mo further increased from 0.8 wt.% to 1.2 wt.%, the SCC resistance decreased. Based on these results, it could be deduced that the specimen III<sub>G</sub> (0.1 wt.% Cu and 1.5 wt.% Mo) was susceptible to the SCC. Moreover, based on the results of I<sub>A</sub>, I<sub>B</sub> and I<sub>C</sub> obtained in section 3.1.1, it was found that the Cu addition was harmful to the SCC resistance, suggesting that both the specimens III<sub>F</sub> (0.2 wt.% Cu and 1.5 wt.% Mo) and III<sub>E</sub> (0.4 wt.% Cu and 1.5

wt.% Mo) were sensitive to the SCC. On the other hand, it could be deduced that III<sub>A</sub> steel with 0.4 wt.% Cu and without Mo would be insensitive to SCC, according to the result of specimen II<sub>A</sub> (0.4 wt.% Cu and 0.4 wt.% Mo) without SCC failure. Thus, with less Cu content but without Mo addition, III<sub>B</sub> III<sub>C</sub> and III<sub>D</sub> steels were also safe in boiling magnesium chloride solution after 720 h.

3.1.4 SCC morphology analysis

Fig.1 showed the optical images of tested samples I<sub>C</sub>, II<sub>A</sub>, II<sub>H</sub> and III<sub>H</sub> without SCC after 100h immersion in 42 wt.% boiling MgCl<sub>2</sub> solution. Although some black oxide products could be found on the specimen surface, there was no SCC occurred in I<sub>C</sub>, II<sub>A</sub>, II<sub>H</sub> and III<sub>H</sub> steels. Fig. 2 revealed the optical images of tested samples I<sub>A</sub>, I<sub>B</sub> and II<sub>G</sub> with SCC after 24 h immersion in 42 wt.% boiling MgCl<sub>2</sub> solution. It could be figured out that severe SCC occurred in I<sub>A</sub>, I<sub>B</sub> and II<sub>G</sub> steels, and the cracks mainly started at the edge of the U-shaped specimens, and expanded along locations of the maximum tensile stress.



**Figure 1.** Macro-morphology of tested samples (I<sub>C</sub>, II<sub>A</sub>,II<sub>H</sub> and III<sub>H</sub>) without SCC after 100h immersion in 42 wt.% boiling MgCl<sub>2</sub> solution

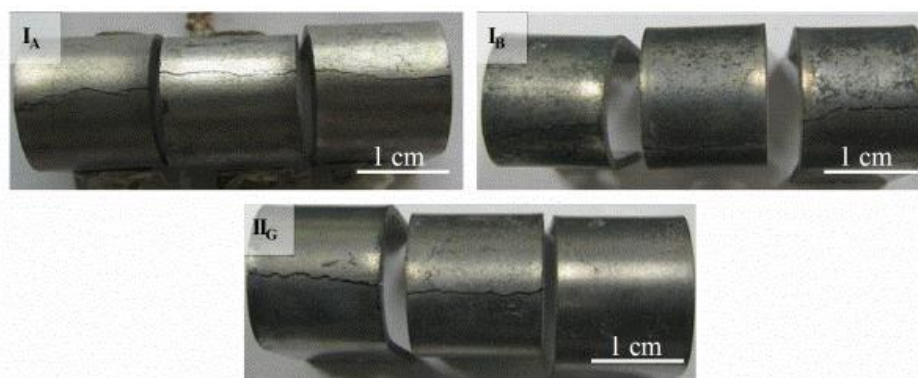


**Figure 2.** Macro-morphology of tested samples (I<sub>A</sub>, I<sub>B</sub> and II<sub>G</sub>) with SCC after 24h immersion in 42 wt.% boiling MgCl<sub>2</sub> solution

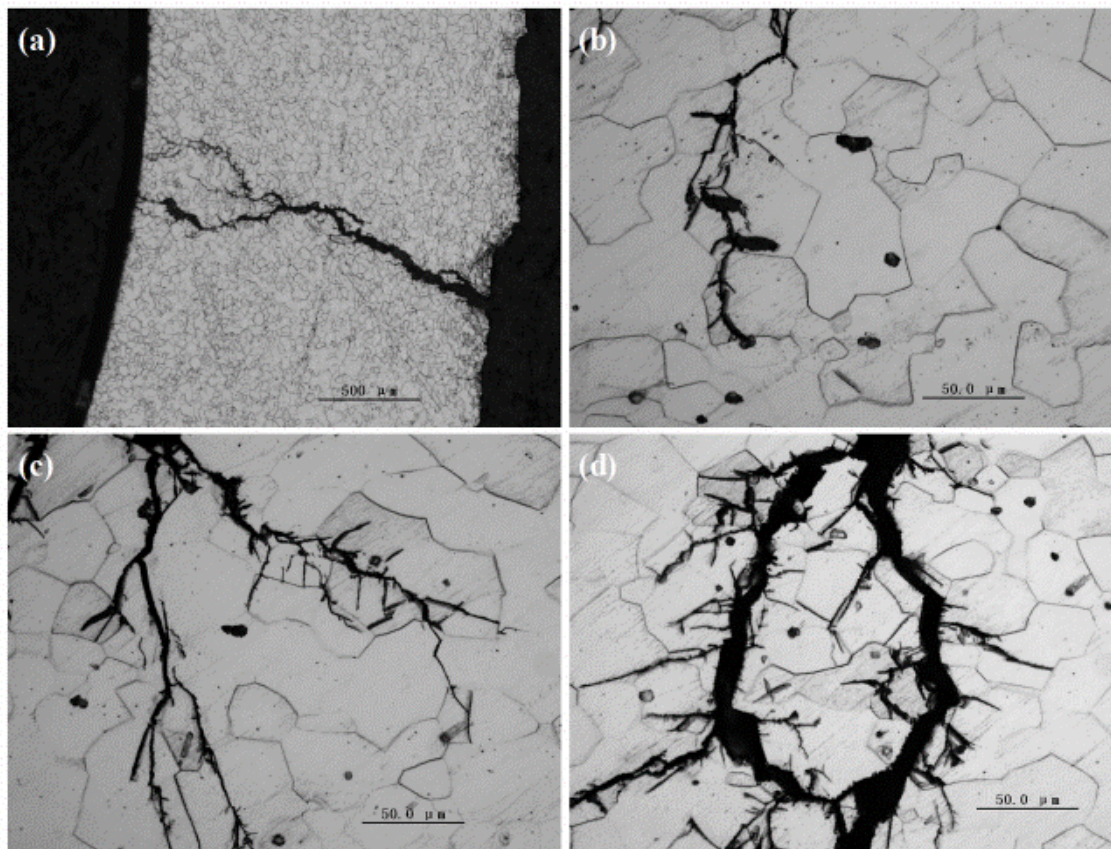


**Figure 3.** SCC micro-morphologies of ultra-pure ferritic stainless steels (a-b) I<sub>A</sub>; (c) I<sub>B</sub>; (d) II<sub>G</sub>

Finally, the surface morphology of the ultra-pure FSSs surfaces after SCC tests was studied by optical microscopy. Fig. 3 demonstrated the optical images of the fracture morphology of the I<sub>A</sub> I<sub>B</sub> and II<sub>G</sub> FSSs. The fracture of these steels was featured by a mixture of intergranular and transgranular fracture, but mostly transgranular fracture. Most of the stress corrosion cracks extended along certain direction straightly in the grain and always terminated at the grain boundary. There were many secondary cracks for all the three steels around the main cracks. The SCC behavior was strongly influenced by the synergy effect of high Mo and Cu content.

### 3.1.5 Quantitative effect of Mo and Cu contents on SCC

In order to directly study the quantitative effect of Mo and Cu contents on SCC of ultra-pure ferritic stainless steels, Fig. 4 was plotted by combining the SCC results in Table 3 and the composition of specimens in Table 1. It is worth noticing that the SCC occurred in the ultra-pure ferritic stainless steels with both Cu and Mo addition. When Cu and Mo contents were all less than 0.4 wt.%, the steels could be immune to the SCC failure. The ones with more than 0.8 wt.% but less than 1.5 wt.% Mo and more than 0.2 wt.% Cu were sensitive to the SCC.

Fig. 4 showed the quantitative effect of Mo and Cu on the SCC sensitivity of ultra-pure ferritic stainless steels. The whole diagram was divided into three regions 1, 2, and 3 by two curves (A and B). Curve A connected the points which represented the steels without SCC cracks after 720 h test, and Curve B indicated the steels with SCC cracks within 720 h. These three regions and two curves could clarify the quantitative effect of Mo and Cu on the SCC of ultra-pure ferritic stainless steels. The stainless steels with Mo and Cu additions in the region 1 under the curve A would be immune to the SCC, and the ones with the Mo and Cu additions in the region 3 above the curve B would be sensitive to the SCC failure. Meanwhile, the ones in the region 2 between the curves A and B might had two possibilities, to occur SCC or to be safe in boiling 42 wt.% MgCl solution within 720 h. In this case, with the additions of Mo and Cu decreasing, far away from curve B, these stainless steels might be more possible to be immune to the SCC. It could be obtained that the stress corrosion cracking sensitivity of the steels with more addition of Mo and Cu was higher by comparisons.

For ultra-pure ferritic stainless steels, the precipitation of  $\epsilon$ -Cu phases in matrix and grains could induce a decrease of the passive film stability with Cu addition increasing, and the pitting corrosion was easy to start at the interface areas between inclusions and the matrix. At the same time, there was a common opinion that the film was a porous oxide containing higher oxidation states of Mo [29]. Pits on the passive film could be the initiation of SCC. At the crack initiation stage, many weak sites, such as grain boundaries, twin boundaries, edges of corrosion grooves parallel to stress, and micropits at maximum stress area could also be the SCC initiation. Once micro-crack existed, it would act as the anodic with a small working area, while the base metal covered with complete film would act as the cathode [30-35]. The geometrical feature of the sample surface could affect the current density distribution during the chemical reactions, thus influencing the corrosion rate [36-39]. The big area ratio of cathode to anode accelerated the solution rate of the micro-crack, leading to the further crack growth. Thus, the specimens with more addition of Mo and Cu were more susceptible to SCC. Moreover, the morphology of SCC initiated from pitting of  $\epsilon$ -Cu phase was mostly intergranular [29].

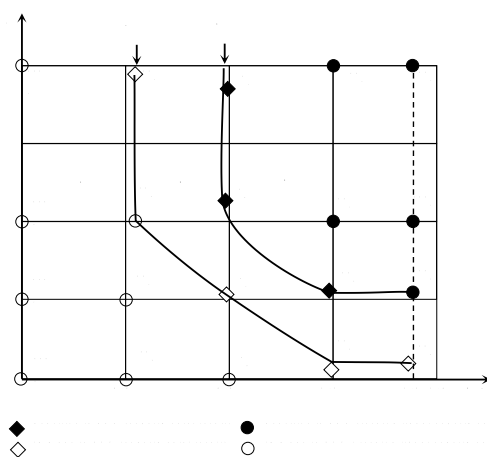


**Figure 4.** Quantitative effect of Mo and Cu on the SCC of ultra-pure ferritic stainless steels

3.2 Effect of Mo and Cu on pitting corrosion resistance

In order to study the effects of Mo and Cu on pitting corrosion resistance of ultra-pure ferritic stainless steel, four steels, II<sub>A</sub> (0.4 wt.% Mo, 0.4 wt.% Cu), II<sub>B</sub> (0.4 wt.% Mo, 0.2 wt.% Cu), II<sub>G</sub> (1.2 wt.% Mo, 0.1 wt.% Cu) and II<sub>H</sub> (1.2 wt.% Mo, without Cu) were chosen to be tested by cyclic salt spray test, polarization curves and FeCl<sub>3</sub> immersion test. Fig. 5 displayed the corrosion morphology of ultra-pure ferritic stainless steels after 240 h cyclic salt spray test. From the corrosion morphology, it could be found that only slight corrosion occurred on the surfaces for the four steels. However, specimens II<sub>A</sub> and II<sub>B</sub> with 0.4 wt.% Mo suffered from more severe corrosion compared to specimens II<sub>G</sub> and II<sub>H</sub> containing 1.2 wt.% Mo, which suggested unbroken surfaces with few rust trace.

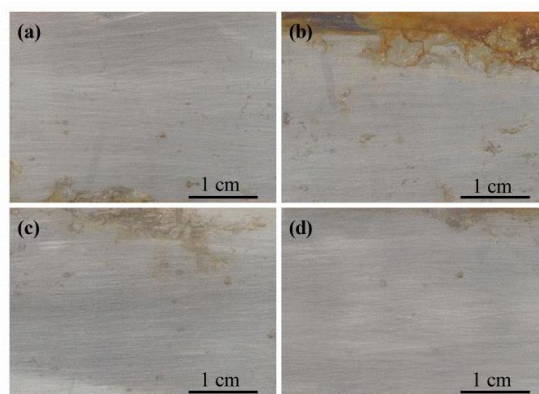


**Figure 5.** Corrosion macro-morphology of ultra-pure ferritic stainless steels after 240 h cyclic salt spray test (a) II<sub>A</sub> (0.4% Mo 0.4% Cu) ; (b) II<sub>B</sub> (0.4% Mo 0.2% Cu) ; (C) II<sub>G</sub> (1.2% Mo 0.1% Cu) ; (d) II<sub>H</sub> (1.2% Mo without Cu)

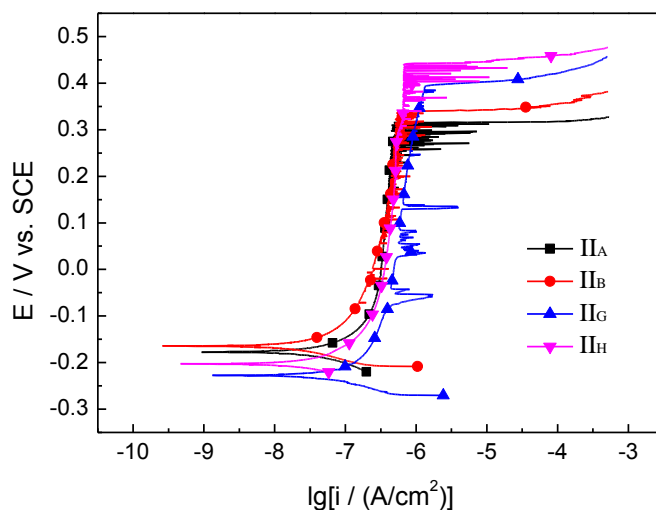


**Figure 6.** Effect of Mo and Cu on polarization curves for ultra-pure ferritic stainless steels in 3.5 wt.% NaCl solutions

**Table 4.** Corrosion parameters of ultra-pure ferritic stainless steels II<sub>A</sub>, II<sub>B</sub>, II<sub>G</sub> and II<sub>H</sub>.

Materials	$i_{corr}/(A/cm^2)$	$E_{corr}/V$	Anodic Tafel slope / (V/dec)	Cathodic Tafel slope / (V/dec)	$E_b/V$	$E_b-E_{corr}/V$
II <sub>A</sub>	1E-9.031	-0.178	0.135±0.002	0.034±0.003	0.316	0.494
II <sub>B</sub>	1E-9.585	-0.164	0.233±0.005	0.030±0.004	0.356	0.520
II <sub>G</sub>	1E-8.881	-0.227	0.246±0.003	0.036±0.003	0.421	0.648
II <sub>H</sub>	1E-9.330	-0.203	0.357±0.001	0.021±0.005	0.460	0.663

Fig. 6 demonstrated the potentiodynamic polarization curves of the ultra-pure ferritic stainless steels II<sub>A</sub> and II<sub>B</sub> with 0.4 wt.% Mo, II<sub>G</sub> and II<sub>H</sub> with 1.2 wt.% Mo. Corresponding corrosion parameters were listed in Table 4. The corrosion current density of the four specimens increased on the order of II<sub>B</sub> < II<sub>H</sub> < II<sub>A</sub> < II<sub>G</sub>, while the corrosion potential increased on the order of II<sub>G</sub> < II<sub>H</sub> < II<sub>B</sub> < II<sub>A</sub>. The pitting broken potentials ( $E_b$ ) of specimens II<sub>A</sub> and II<sub>B</sub> were 0.316 and 0.356 V, whereas specimens II<sub>G</sub> and II<sub>H</sub> steels were 0.421 and 0.460 V, respectively. Therefore, the  $E_b$  of specimens increased on the order of II<sub>A</sub> < II<sub>B</sub> < II<sub>G</sub> < II<sub>H</sub>. The higher  $E_b$  values of specimens II<sub>G</sub> and II<sub>H</sub> suggested the higher pitting corrosion resistance than specimens II<sub>A</sub> and II<sub>B</sub>. The passivation region of specimens was evaluated by  $E_b-E_{corr}$ . It also could be seen that the passivation ability of the specimens increased on the order of II<sub>A</sub> < II<sub>B</sub> < II<sub>G</sub> < II<sub>H</sub>. It could be found that with the Mo addition, the values of  $E_b$  and  $E_b-E_{corr}$  increased, indicating that Mo could improve the pitting corrosion resistance and passivation ability. Besides, it is worth noticing that a decrease in the pitting corrosion resistance and passivation ability were found with the increasing Cu content in ferritic stainless steels containing 0.4 wt.% Mo and 1.2 wt.% Mo. Therefore, the addition of Cu was harmful to the pitting corrosion resistance of ultra-pure ferritic stainless steels.

Pitting corrosion morphologies after immersion test of ultra-pure ferritic stainless steels in FeCl<sub>3</sub> solution at 35°C were shown in Fig. 7, and the results of corrosion rates were listed in Table 5. It could be observed that severe pitting corrosion occurred on the specimens II<sub>A</sub> and II<sub>B</sub>, and most of the pits located at the edges of the specimen, and some pits could be found inside the specimen. In contrast to II<sub>A</sub> and II<sub>B</sub> with 0.4 wt.% Mo, less pitting holes could be found inside the II<sub>G</sub> and II<sub>H</sub> specimens.

As shown in Table 5, pitting corrosion rates of II<sub>A</sub>, II<sub>B</sub>, II<sub>G</sub> and II<sub>H</sub> steels in 6 wt.% FeCl<sub>3</sub> solution were 11.94, 10.81, 6.82 and 5.53 g/(m<sup>2</sup>·h), respectively. The results showed that the specimens II<sub>G</sub> and II<sub>H</sub> with 1.2 wt.% Mo had lower corrosion rate than the specimens of II<sub>A</sub> and II<sub>B</sub> with 0.4 wt.% Mo, suggesting that the addition of Mo increased the pitting corrosion resistance. Meantime, the corrosion rates of specimens II<sub>H</sub>, II<sub>G</sub>, II<sub>B</sub> and II<sub>A</sub> showed an increasing trend with the Cu content increasing.

The Cu addition reduced the pitting broken potential and increased the corrosion rate in chloride containing environment, suggesting a decrease of the corrosion resistance. Therefore, the addition of Cu was harmful for the pitting corrosion resistance of II<sub>G</sub>, II<sub>B</sub> and II<sub>A</sub> steels, which might be attributed to that the ε-Cu phases precipitated in grain boundaries and grains of ferritic stainless steels. The solubility of Cu in ferrite was low, about ~0.2 wt.%, so with the increasing Cu content, the precipitation of the ε-phase might occur at grain boundaries and grains in ferrite stainless steels [40-

41]. It has been reported that the presence of the  $\epsilon$ -phase in ferrite could increase the hardness of ferritic stainless steels [42]. However, the dispersed inclusions of this phase could negatively influence the stability of passive film of stainless steels and therefore increase the susceptibility of ferrite to the pitting corrosion.

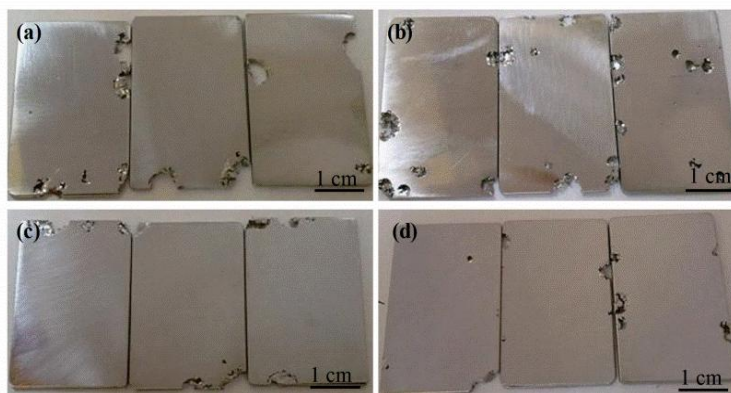


**Figure 7.** Pitting corrosion macro-morphologies of ultra-pure ferritic stainless steels in  $\text{FeCl}_3$  solutions at  $35^\circ\text{C}$  after 24 h immersion (a)  $\text{II}_A$ ; (b)  $\text{II}_B$ ; (c)  $\text{II}_G$ ; (d)  $\text{II}_H$

**Table 5.** Corrosion rate of ultra-pure ferritic stainless steels in  $\text{FeCl}_3$  solutions at  $35^\circ\text{C}$

Materials	Corrosion rate / $\text{g}/(\text{m}^2 \cdot \text{h})$	Mean value / $\text{g}/(\text{m}^2 \cdot \text{h})$	Materials	Corrosion rate / $\text{g}/(\text{m}^2 \cdot \text{h})$	Mean value / $\text{g}/(\text{m}^2 \cdot \text{h})$
$\text{II}_A$	13.338	11.94	$\text{II}_G$	6.029	6.82
	11.684			7.264	
	10.791			7.165	
$\text{II}_B$	11.472	10.81	$\text{II}_H$	5.367	5.53
	11.037			5.190	
	9.924			6.041	

#### 4. CONCLUSIONS

In order to quantitate the effect of alloying Cu and Mo on the stress corrosion cracking and pitting corrosion of ferritic stainless steels in chloride media, twenty ultra-pure ferritic stainless steels with 22 wt.% Cr but different Cu and Mo additions were designed. Eight kinds of them were smelted and their SCC behavior was evaluated. Besides, pitting corrosion behavior of four kinds of specimens was measured. Conclusions were as follows:

(1) When Cu and Mo contents were all less than 0.4 wt.%, the steels could be immune to the SCC failure. The ones with more than 0.8 wt.% and 0.2 wt.% Cu together were sensitive to the SCC.

(2) The quantitative effect of Mo and Cu addition on the SCC of ultra-pure ferritic stainless steel was given in a whole graph. The steels with more addition of Mo and Cu were more susceptible to SCC.

(3) With the increasing Mo content, the pitting corrosion resistance increased remarkably in chloride containing environment. The addition of Cu reduced the pitting corrosion resistance of ultra-pure ferritic stainless steel due to the precipitation of  $\epsilon$ -Cu phase.

## References

1. X.M. You, Z.H. Jiang, H.B. Li, *J. Iron. Steel Res. Int.*, 14 (2007) 24.
2. Y.T. Shan, X.H. Luo, X.Q. Hu, S. Liu, *J. Mater. Sci. Technol.*, 27 (2011) 352.
3. C.T. Bi, *Iron and Steel* 31 (1996) 74 (in Chinese).
4. X. Wei, J.H. Dong, J. Tong, Z. Zheng, W. Ke, W. *Int. J. Electrochem. Sci.*, 8 (2013) 887.
5. J.Y. Hong, Y.T. Shin, H.W. Lee, *Int. J. Electrochem. Sci.*, 9 (2014) 7325.
6. R.A. Marques, S.O. Rogero, M. Terada, E.F. Pieretti, I. Costa, *Int. J. Electrochem. Sci.*, 9 (2014) 1340.
7. A. Samide, B. Tutunaru, A. Moanță, C. Ionescu, C. Tigae, A.C. Vladu, *Int. J. Electrochem. Sci.*, 10 (2015) 4637.
8. C.J.O. Alonso, M.A. Lucio-Garcia, I.A. Hermoso-Diaz, J.G. Chacon-Nava, A. Martinez-Villafañe, J.G. Gonzalez-Rodriguez, *Int. J. Electrochem. Sci.*, 9 (2014) 6717.
9. I.U.H. Toor, *Int. J. Electrochem. Sci.*, 9 (2014) 2737.
10. K. Sugimoto, Y. Sawada, *Corros. Sci.*, 17 (1977) 425.
11. Z. Szklarska-Smialowska, *Pitting Corrosion of Metals*, National Association of Corrosion Engineers, Houston, 1986. p.147.
12. Ya.M. Kolotyркиn, L.I. Freiman, in: *Korroziya i Zashchita ot Korroziy*, vol. 5, Izd. WINITI, Moscow, 1978, p.5
13. R.C. Newman, *Corros. Sci.*, 25 (1985) 331.
14. H. Ogawa, H. Omata, I. Itoh, H. Okada, *Corrosion*, 34 (1978) 53-65.
15. A. Yamamoto, T. Ashiura, E. Kamisaka, *Boshoku Gijutsu*, 35 (1986) 448-454.
16. H. Watanabe, T. Yoshii, A. Fujii, T. Kanamaru, *Tetsu to Hagane*, 69 (1983) S1502.
17. H. Ohashi, T. Adachi, K. Maekita, *Tetsu to Hagane* 66 (1980) S1309.
18. S.T. Kim, Y.S. Park, *Corrosion*, 63 (2007) 114.
19. A.A. Hermas, K. Ogura, S. Yakagi, T. Adachi, *Corrosion*, 51 (1995) 3.
20. T. Ujiro, S. Satoh, R.W. Staehle, W.H. Smyrl, *Corros. Sci.*, 43 (2001) 2185.
21. A.A. Hermas, K. Ogura, S. Yakagi, T. Adachi, *Corrosion*, 51 (1995) 3.
22. M. Schwind, J. Källqvist, J.O. Nilsson, J. Ågren, H.-O. Andrén, *Acta Mater.*, 48 (2000) 2473.
23. M. Seo, G. Hultquist, C. Leygraf, N. Sato, *Corros. Sci.*, 26 (1986) 949.
24. J. Shu, H.Y. Bi, X. Li, Z. Xu, *Corros. Sci.*, 57 (2012) 89.
25. ASTM G36-94. Standard Practice for Evaluating Stress-Corrosion-Cracking Resistance of Metals and Alloys in a Boiling Magnesium Chloride Solution, Annual Book of ASTM Standards; ASTM International: West Conshohocken, PA, USA, 2000. vol. 03.02. pp. 134.
26. ASTM G30-97. Standard Practice for Making and Using U-Bend Stress-Corrosion Test Specimens, Annual Book of ASTM Standards; ASTM International: West Conshohocken, PA, USA, 2009. vol. 03.02.
27. GB/T 20854-2007. Corrosion of metals and alloys-Accelerated testing involving cyclic exposure to salt mist, "dry" and "wet" condition.

28. ASTM G48-03. Standard Test Methods for Pitting and Crevice Corrosion Resistance of Stainless Steels and Related Alloys by Use of Ferric Chloride Solution, Annual Book of ASTM Standards; ASTM International: West Conshohocken, PA, USA, 2003. vol. 03.02. pp. 191.
29. R.J. Brigham, *Corrosion*, 28 (1972) 177.
30. C. Zhong, F. Liu, Y.T. Wu, J.J. Le, L. Liu, M.F. He, J.C. Zhu, W.B. Hu, *J. Alloy. Compd.*, 520 (2012) 11.
31. C. Zhong, W.B. Hu, Y.M. Jiang, B. Deng, J. Li, *J. Coat. Technol. Res.*, 8 (2011) 107.
32. J.J. Le, L. Liu, F. Liu, Y.D. Deng, C. Zhong, W.B. Hu, *J. Alloy. Compd.*, 610 (2014) 173.
33. C. Zhong, M.F. He, L. Liu, Y.T. Wu, Y.J. Chen, Y.D. Deng, B. Shen, W.B. Hu, *J. Alloy. Compd.*, 504 (2010) 377.
34. C. Zhong, M.F. He, L. Liu, Y.J. Chen, B. Shen, Y.T. Wu, Y.D. Deng, W.B. Hu, *Surf. Coat. Technol.*, 205 (2010) 2412.
35. C. Zhong, X. Tang, Y.F. Cheng, *Electrochim. Acta*, 53 (2008) 4740.
36. J. Liu, X.T. Du, Y. Yang, Y.D. Deng, W.B. Hu, C. Zhong, *Electrochem. Commun.*, 58 (2015) 6.
37. J. Liu, C. Zhong, X.T. Du, Y.T. Wu, P.Z. Xu, J.B. Liu, W.B. Hu, *Electrochim. Acta*, 100 (2013) 164.
38. J. Liu, W. Hu, C. Zhong, Y.F. Cheng, *J. Power Sources*, 223 (2013) 165.
39. C. Zhong, W.B. Hu, Y.F. Cheng, *J. Power Sources*, 196 (2011) 8064.
40. A. Mazurkiewicz, J. Glowina, J. Banas, *Materials Science Forum*, 185-188 (1995), 749.
41. F.B. Pickering, *The Metal Society*, 1984.
42. J. Banas, A. Mazurkiewicz, *Mater. Sci. Eng. A.*, 277 (2000) 183.

© 2015 The Authors. Published by ESG ([www.electrochemsci.org](http://www.electrochemsci.org)). This article is an open access article distributed under the terms and conditions of the Creative Commons Attribution license (<http://creativecommons.org/licenses/by/4.0/>).